Surface Science Letters

Adsorbate mobilities on catalyst nanoparticles studied via the angular distribution of desorbing products

V. Johánek [a], M. Laurin [a], J. Hoffmann [a], S. Schauermann [a], A.W. Grant [b], B. Kasemo [b], J. Libuda [a,*], H.-J. Freund [a]

[a] *Department of Chemical Physics, Fritz-Haber-Institut der Max-Planck-Gesellschaft, Faradayweg 4-6, 14195 Berlin, Germany*
[b] *Department of Applied Physics, Chalmers University of Technology, SE-412 96, Göteborg, Sweden*

Abstract

Employing molecular beam methods, we have studied the angular distribution of products desorbing from oxide-supported Pd nanoparticles during catalytic oxidation of CO. A large range of particle sizes was covered by combining preparation techniques based on (1) metal evaporation and growth and (2) electron beam lithography. Whereas the CO_2 distribution is symmetric and independent of the reaction conditions on small Pd aggregates, a strong influence of the reactant incidence angles and fluxes was observed for large particles. For the first time, these observations experimentally verify the existence of local reaction rate variations on a catalyst nanoparticle as a consequence of limited adsorbate mobility. Furthermore, the results allow us to extract in situ information about surface diffusion rates.
© 2004 Elsevier B.V. All rights reserved.

Keywords: Catalysis; Surface diffusion; Palladium; Carbon monoxide; Oxidation

In spite of its enormous practical impact on chemical industry and environmental technology, reaction kinetics on heterogeneous catalysts is still poorly understood [1]. The reason for this lack of knowledge is related to the complex surface structure of real catalysts, the coupling of many elementary steps in the overall reaction mechanism and the experimental difficulties arising in structural and kinetic studies on these systems.

In order to overcome these problems, different types of model systems have been developed, which were specifically designed to resemble particular structural and chemical features of real catalysts without having to deal with their full complexity [2–4]. Recently, we started to investigate the surface reaction kinetics on such model catalysts employing molecular beam methods [5]. The use of molecular beams can provide detailed insights into the kinetics and dynamics on heterogeneous catalyst surfaces. Here, the surface mobility of adsorbates represents one aspect, which was recently shown to be of crucial importance for a microscopic understanding of the

reaction kinetics on nano-structured surfaces [6–8]. In case of supported catalysts, typically consisting of nanometer-sized metal particles on an oxide support, surface diffusion can occur, e.g., between different sites or facets on the active particle, and/or between the support and the particle. Unfortunately, there is very limited experimental information available on the surface mobility of reactants under reaction conditions. This is because in practice there are hardly any experimental tools, which are capable of providing such data under well-controlled conditions. Potentially, methods such as fast scanning tunneling microscopy [9] or photoelectron microscopy [10] could be applied, however, these techniques suffer severe limitations with respect to the types of surfaces and the experimental conditions which can be accessed.

In a recent publication we suggested the use of angular resolved measurements in order to determine local reaction rates on supported model catalysts [11]. Unfortunately, the limited range of the particle sizes precluded the identification of clear angular dependent effects. In the present Letter, we extend our approach to model catalysts prepared by means of electron beam lithography (EBL) and, in this manner, expand the accessible range of particle sizes to significantly larger aggregates. As a result, we were now able to experimentally observe the predicted local variations of the reaction rates for the first time and could extract information on the surface mobility of adsorbates on nm-sized particle under reaction conditions.

The two model catalysts used in this work are shown in Fig. 1a and b.

Sample A: Large Pd particles (diameter: 500 nm; height: 450 nm) arranged in an hexagonal array were prepared by means of EBL on a SiO_2 film on Si(1 0 0) at the MC2 Laboratory, Chalmers University (Göteborg, Sweden) (see [12] for general information, details will be given elsewhere [13]). After 'lift off' of the EBL resist, the sample was cleaned and "chemically annealed" by applying oxidation/reduction cycles in O_2/Ar and H_2/Ar mixtures, respectively. Subsequently, the samples were transported to the Fritz-Haber-Institute (Berlin), where the reactivity measurements were performed in an ultrahigh vacuum (UHV) molecular beam system described previously [14]. Prior to the experiments, the sample was cleaned by extended oxygen treatment and heating cycles. The cleanliness of the sample was checked via measurements of the CO desorption behavior and the oxygen adsorption capacity as quantified by CO titration [13].

Sample B: Small Pd particles (diameter: 6 nm; height: 2 nm) were prepared by means of metal evaporation and growth directly in the UHV molecular beam apparatus [5]. As a model support, a thin Al_2O_3 film prepared on a NiAl(110) single crystal was employed. The Pd model catalyst was investigated in a series of previous studies and we refer to the literature for details concerning the preparation, the geometric and electronic structure and the adsorption properties [15]. It should be noted that both supports used in this work, alumina and silica, show only weak interactions with deposited Pd metal. Thus, we do not expect the adsorption or reaction properties of the particles to by significantly affected by support effects.

The experimental setup used in this work is displayed in Fig. 1c. The reactants, CO and O_2, were supplied via up to three molecular beam sources, allowing individual control of the incidence angles and fluxes of the reactants. In the following, the intensity ratio of the beams is described by the fraction of CO in the impinging gas flux $x_{CO} = F_{CO}/(F_{CO} + F_{O_2})$ with F_{CO} and F_{O_2} representing the CO and oxygen flux densities, respectively. Two experimental geometries were chosen such that by using a single or a double CO beam, the incident CO flux was nearly symmetric with respect to the plane which is perpendicular to the scattering plane and contains the sample normal. The key point in the experiment is the O_2 incidence angle, which was chosen to be tilted with respect to the surface normal. As a result, different parts of the surface of an individual particle were exposed to different local fluxes of O_2; some parts were exposed directly to incident O_2, while other parts were shadowed and not exposed at all. It thus depends on the rate of surface diffusion of adsorbed oxygen, whether these differences in reactant flux lead to local variations of the steady-state coverages and reaction rates (note that CO
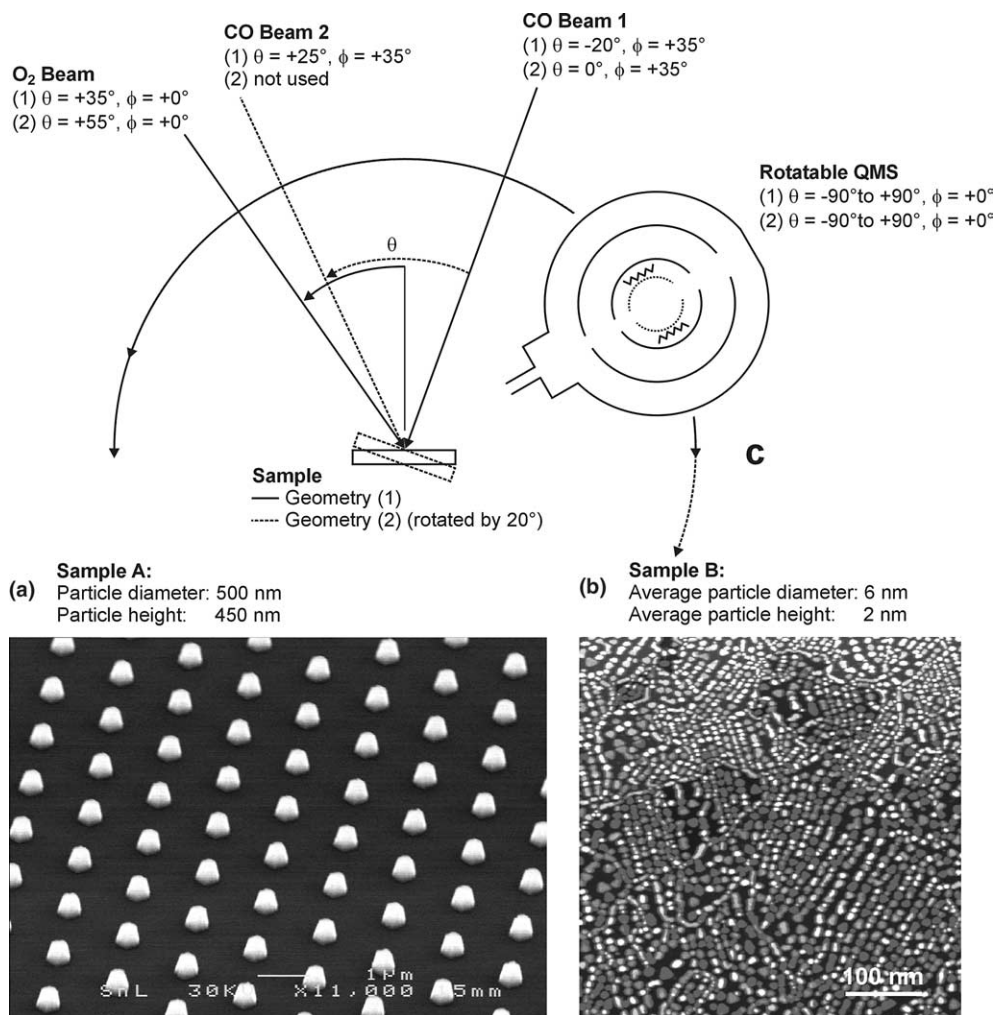
Fig. 1. (a) Scanning electron microscopy (SEM) image of the Pd particles on $SiO_2/Si(100)$, prepared by electron beam lithography (EBL) (particle density 0.5×10^8 particles cm^{-2}); (b) scanning tunneling microscopy (STM) image of the Pd particles on $Al_2O_3/NiAl(110)$, from [15], prepared by in situ evaporation and growth (particle density 1.0×10^{12} particles cm^{-2}); (c) experimental set-up used for the angular resolved reaction rate measurements. The reactants were supplied via molecular beams of CO with variable intensity between 1×10^{14} cm^{-2} s^{-1} and 2×10^{15} cm^{-2} s^{-1} and a molecular beam of O_2 beam with an intensity of 4–6×10^{14} cm^{-2} s^{-1}.

diffusion is always fast compared to oxygen diffusion, see [16]). For the angular resolved rate measurements, we take advantage of the fact that the interaction of the product CO_2 on Pt-group metals is weak, leading to almost immediate desorption. As the maximum desorption rate is always directed along the local surface normal, we expect that the CO_2 angular distribution directly reflects the distribution of local reaction rates over the differently oriented microfacets of the particle surface (note that an exact quantitative analysis is complicated by the fact that the angular distribution from a given site sensitively depends on the presence of co-adsorbed reactants [17,18]).

In our experiments we measured the angular distribution of CO_2 using a differentially pumped rotatable mass spectrometer (Fig. 1c, [14]). A summary of the corresponding data is displayed in Figs. 2 and 3.

CO$_2$ Angular Distribution:

a - Sample A (500 nm), Geometry (1)

c - Total CO$_2$ Production Rate
Sample A (500 nm), Geometry (1)

b - Sample A (500 nm), Geometry (2)

d - Sample B (6 nm), Geometry (1)
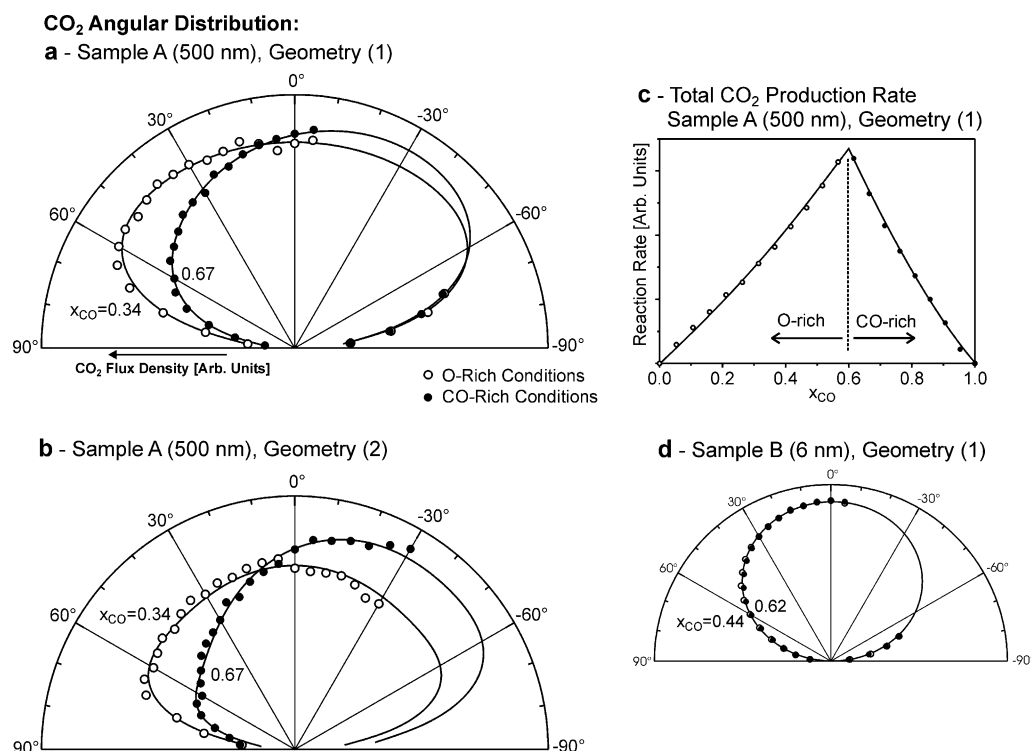
Fig. 2. (a,b) Comparison of the angular distribution of CO$_2$ desorbing under steady-state conditions from the Pd particles of sample A under CO-rich (solid symbols) and O-rich (open symbols) conditions. Note that for both experimental geometries, the O$_2$ beam is blocked for a range of detection angles precluding the acquisition of the corresponding data points. Isotopically labeled [13]CO was used in order to reduce the noise level. The data were corrected for the angular acceptance function of the detector as described earlier [14]; (c) integral steady-state reaction rate as a function of the CO fraction in the incident gas flux x_{CO} measured for CO oxidation on sample A at 465 K; (d) angular distribution of CO$_2$ desorbing under steady-state conditions from the Pd particles of sample B under CO-rich (solid symbols) and O-rich (open symbols) conditions.

In the first step, we focus on the influence of the reactant fluxes on the angular product (CO$_2$) distributions. A typical behavior of the total reaction rate as a function of x_{CO} is displayed in Fig. 2c. Two reaction regimes can be clearly distinguished, denoted in the following as the CO-*rich* and the O-*rich* regimes. The corresponding steady-states are characterized by high CO and low O coverages and vice versa. Analyzing the corresponding CO$_2$ patterns for sample A (500 nm, Fig. 2a and b) we observe a strong dependence on the reaction conditions: (a) under O-rich conditions ($x_{CO} = 0.34$) the angular distributions are symmetric and (b) under CO-rich conditions ($x_{CO} = 0.67$) the distributions are asymmetric with a considerably enhanced CO$_2$ production on the side facing the O$_2$

beam. In contrast to this, the angular distributions for sample B (6 nm, Fig. 2d) show no dependence on the reaction conditions.

These results clearly demonstrate that oxygen diffusion over the particle is sufficiently fast to result in complete equilibration of the local O coverage for sample A (500 nm) under O-rich conditions, whereas under CO-rich conditions no complete equilibration occurs. In contrast to this, there is complete equilibration in the case of sample B (6 nm) under all reaction conditions (it should be noted that in spite of the lower aspect ratio for sample B as compared to sample A, the majority of surface atoms is still located on the side facets. Therefore, differing reaction rates on the side facets should yield a significant

CO$_2$ Angular Distribution - Sample A (500 nm)

**X$_{CO}$ Dependence
(T = 465 K)**
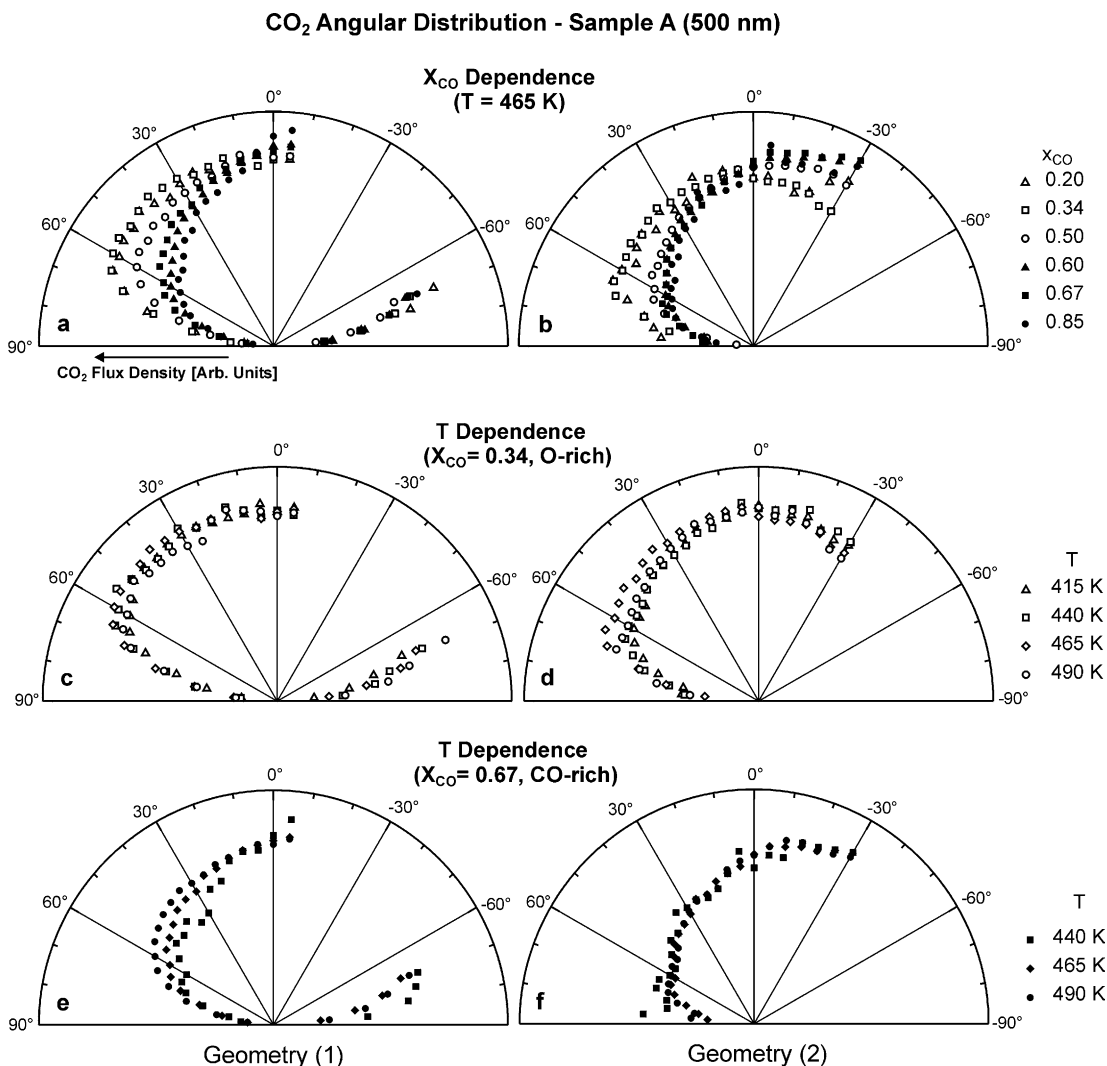
Fig. 3. (a,b) Angular distribution of CO$_2$ desorbing under steady-state conditions from the Pd particles of sample A as a function of the CO fraction in the incident gas flux x_{CO}; (c,d) angular distribution of CO$_2$ under O-rich reaction conditions as a function of surface temperature; (e,f) angular distribution of CO$_2$ under CO-rich reaction conditions as a function of surface temperature.

asymmetry of the CO$_2$ angular distribution also for sample B).

In the next step we analyze the dependence of the CO$_2$ angular distribution on x_{CO} and on the surface temperature (T_S) for sample A (500 nm) in more detail (see Fig. 3). It is found that the CO$_2$ distribution switches within a narrow x_{CO} range from a symmetric to an asymmetric shape (Fig. 3a,b). The switching occurs at the transition point from the O-rich to the CO-rich region. In contrast

to the pronounced influence of x_{CO}, the angular CO$_2$ distributions exhibit no detectable temperature dependence both under O-rich ($x_{CO} = 0.34$, Fig. 3c,d) and under CO-rich ($x_{CO} = 0.67$, Fig. 3c,d) conditions.

The key quantity, which determines the equilibration of the reactant coverages on a particle is the oxygen diffusion length L_d during the surface residence time τ_O. For adsorbed oxygen, $\tau_O = \theta_O$ TOF^{-1} is determined by the steady-state coverage

θ_O and the reaction rate TOF (turnover frequency, product molecules formed per active surface atom and time), with both values sensitively depending on the reaction conditions. At this point, further insight can be obtained from microkinetic simulations. Using a mean field model described previously [19], the steady state TOF values were fitted to the experimental data (Fig. 4a) and, subsequently, τ_O was calculated (Fig. 4b). As suggested by the angular resolved experiments, a strong dependence of the residence time on x_{CO} is found, together with a sudden decrease at the transition point between the O- and CO-rich regimes. The latter effect is due to the rapidly declining θ_O upon crossing the kinetic phase transition between the two regimes. Contrary to the strong influence of x_{CO}, the dependence of the residence time on T_S is moderate. This is due to
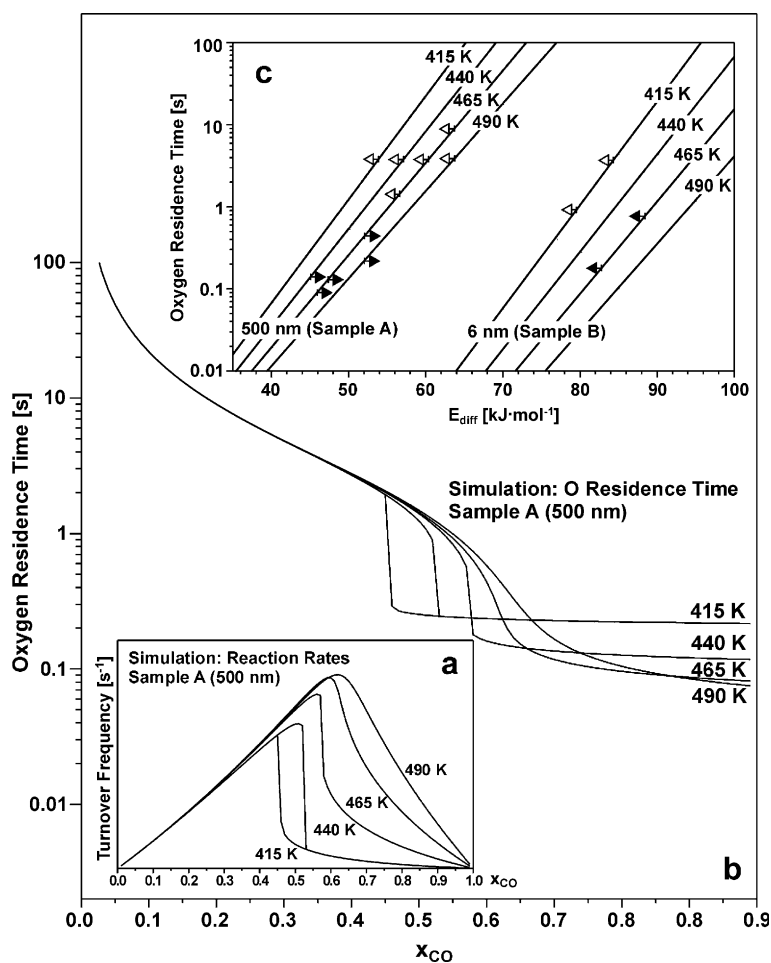
Fig. 4. (a) Simulation of the steady state reaction rate on the Pd particles of sample A as obtained from a fit of the microkinetic model described in [19] to the experimental data ($E_{des} = 142$ kJ mol^{-1}; $\nu_{des} = 4 \times 10^{14}$ s^{-1}; $\alpha_{des} = 0.12$; $S_{CO} = 0.7$; $C_{T_S} = 0.3$; $E_{LH} = 53$ kJ mol^{-1}; $\nu_{LH} = 5 \times 10^7$ s^{-1}; $S_O = 1.0 - 7.4 \times 10^{-4}T_S$; see [19]. Note that at low reaction temperature a bistable behavior occurs, which will be discussed in detail elsewhere [21]); (b) oxygen residence times as calculated from the simulation; (c) oxygen residence times required to provide a diffusion length in the order of the different particle diameters assuming an Arrhenius type behavior of the diffusion coefficient with different activation barriers and a 'normal' pre-exponential factor of $D_0 = 10^{-3}$ cm^2 s^{-1}. The arrows indicate upper and lower limits for the diffusion barrier under CO-rich (solid symbols) and O-rich (open symbols) as derived from the angular resolved data.

SURFACE SCIENCE
LETTERS

two competing effects: the increasing reaction rate with increasing T_S is partially compensated by an increasing θ_O. The latter is the consequence of a decreasing CO coverage at higher T_S due to faster desorption and reaction, resulting in reduced inhibition of O adsorption.

Based on the results from the angular resolved rate measurements and the microkinetic simulations, some information on the oxygen diffusion barrier E_{diff} can be obtained. For this purpose, we estimate the surface residence times required for diffusion across a particle based on the Einstein relation as a function of particle size, surface temperature and diffusion activation energy E_{diff}. In the corresponding plot in Fig. 4c, upper und lower limits for the activation barriers are indicated, as derived from the angular dependent behavior at the different reaction conditions and particle sizes. Under CO-rich reaction conditions a lower limit of 50 ± 5 kJ mol^{-1} (sample A) and an upper limit of 85 ± 5 kJ mol^{-1} (sample B) is obtained for E_{diff}, whereas under O-rich reaction conditions we find an upper limit of 60 ± 5 kJ mol^{-1} (sample A).

So far, no quantitative experimental data for oxygen diffusion on Pd single crystal surfaces is available, which could be compared to the present results. However, the value is in good agreement with recent theoretical investigations, predicting a diffusion barrier of 54 kJ mol^{-1} on Pd(1 1 1) [20]. Nonetheless, such comparisons should be treated with care as the present measurements correspond to a surface 'under reaction conditions', i.e., at high oxygen or CO coverage, whereas the calculations are typically performed in the low coverage limit. At high coverages adsorbate interactions are expected to significantly influence the diffusion activation energies. In addition, it has to be taken into account that on a metal nanoparticle there might be significant contributions to the effective diffusion rates from particle specific sites such as e.g., step, edges, and defects.

In summary, we have studied the steady-state angular distribution of CO_2 desorbing during CO oxidation from oxide-supported Pd nanoparticles. For large particles (500 nm, prepared by electron beam lithography), evidence for local reaction rate variations due to the limited surface mobility of adsorbed oxygen is presented, whereas on small particles (6 nm, prepared by in situ evaporation and growth) oxygen diffusion is found to be sufficiently fast to result in complete equilibration of adsorbate coverages. On the basis of microkinetic simulations, these variations of the angular distribution of CO_2 are analyzed as a function of particle size, surface temperature and reactant fluxes and are utilized to extract data on surface diffusion rates on the catalyst particles under reaction conditions.

References

[1] J.M. Thomas, W.J. Thomas, Principle and Practice of Heterogeneous Catalysis, VCH, Weinheim, 1997.
[2] C.R. Henry, Surf. Sci. Rep. 31 (1998) 231.
[3] V.P. Zhdanov, B. Kasemo, Surf. Sci. Rep. 39 (2000) 25.
[4] H.-J. Freund, Surf. Sci. 500 (2002) 271.
[5] J. Libuda, H.-J. Freund, J. Phys. Chem. B 106 (2002) 4901.
[6] V.P. Zhdanov, B. Kasemo, Surf. Sci. 405 (1998) 27.
[7] V.P. Zhdanov, B. Kasemo, Phys. Rev. B 55 (1997) 4105.
[8] S. Johansson, L. Österlund, B. Kasemo, J. Catal. 201 (2001) 275.
[9] T. Zambelli, J. Trost, J. Wintterlin, G. Ertl, Phys. Rev. Lett. 76 (1996) 795.
[10] W. Huang, R. Zhai, X. Bao, Langmuir 17 (2001) 3629.
[11] J. Hoffmann, S. Schauermann, J. Hartmann, V.P. Zhdanov, B. Kasemo, J. Libuda, H.-J. Freund, Chem. Phys. Lett. 354 (2002) 403.
[12] K. Wong, S. Johansson, B. Kasemo, Faraday Discuss. 105 (1996) 237.
[13] M. Laurin, V. Johanek, A.W. Grant, B. Kasemo, J. Libuda, H.-J. Freund (in preparation).
[14] J. Libuda, I. Meusel, J. Hartmann, H.-J. Freund, Rev. Sci. Instrum. 71 (2000) 4395.
[15] M. Bäumer, H.-J. Freund, Prog. Surf. Sci. 61 (1999) 127.
[16] E.G. Seebauer, C.E. Allen, Prog. Surf. Sci. 49 (1995) 265.
[17] T. Engel, G. Ertl, Chem. Phys. Lett. 54 (1978) 95.
[18] T. Matsushima, H. Asada, J. Chem. Phys. 85 (1986) 1658.
[19] J. Hoffmann, I. Meusel, J. Hartmann, J. Libuda, H.-J. Freund, J. Catal. 204 (2001) 378.
[20] K. Honkala, K. Laasonen, J. Chem. Phys. 115 (2001) 2297.
[21] V. Johánek, M. Laurin, A.W. Grant, B. Kasemo, C.R. Henry, J. Libuda, Science (in press).